# Zeolite ZnY catalysts prepared by solid-state ion exchange

A. Seidel, G. Kampf, A. Schmidt and B. Boddenberg *

*Lehrstuhl für Physikalische Chemie II, Universität Dortmund, Otto-Hahn-Straße 6, D-44227 Dortmund, Germany*
E-mail: bod@pcii.chemie.uni-dortmund.de

Received 28 November 1997; accepted 12 February 1998

Zeolites ZnY with various overall zinc contents were prepared from mixtures of zeolite $NH_4Y$ and crystalline zinc chloride by solid-state ion exchange. The obtained materials were investigated with carbon monoxide, xenon, and nitrogen adsorption as well as with $^{129}Xe$ NMR and XRF spectroscopy. From the results of these measurements, the zinc cation distributions between the different types of cages of the faujasite framework as well as between the crystallographic positions SIII and SII within the large voids (supercages) were quantitatively determined. The concentrations of zinc cations in the supercages of the presently prepared zeolites are considerably higher than in materials obtained from NaY by conventional wet ion exchange using aqueous zinc salt solutions. Experimental evidence is provided for salt inclusion under certain conditions of preparation.

**Keywords:** zeolite ZnY, solid-state ion exchange, salt inclusion, $^{129}Xe$ NMR spectroscopy, adsorption of carbon monoxide and xenon

## 1. Introduction

Low-coordination transition metal cations stabilized in the voids of zeolites are known to exhibit Lewis-acid properties and are believed to be the active sites for a variety of catalytic conversions [1]. Zeolites ZSM-5 containing zinc cations have been reported to catalyze the dehydrogenation of small paraffins such as ethane, as well as the subsequent aromatization of the *in situ* generated ethylene [2,3]. This catalytic reaction opens an interesting pathway for the production of BTX aromatics from a low-value raw material.

Remarkably, catalytic activity with respect to ethane aromatization has not been observed so far for zinc-exchanged zeolites of the faujasite type (X and Y), although these materials should offer several advantages over Zn/ZSM-5. First, with faujasites smaller Si/Al ratios and thus higher total zinc cation concentrations can be achieved. Second, the rather large pore openings of these aluminosilicates should facilitate the transport of the reactant molecules towards and of the products from the active sites, and so improve the overall kinetics of the catalytic conversion. However, $Zn^{2+}$ cations in ZnY catalysts prepared in the conventional way by contact of NaY with aqueous zinc salt solutions are known to have strong preference for positions in the small zeolite voids ($\beta$-cages, hexagonal prisms) [4–10], which are not accessible to molecules with kinetic diameters greater than 0.3 nm. Significant concentrations of $Zn^{2+}$ cations at the crystallographic sites SIII in the supercages, considered liable for catalytic activity, are only observed at sufficiently high ion exchange levels [4–6]. The conventional preparation of materials with such high zinc content requires economically and ecologically unfavourable process conditions like high ion exchange temperatures and repeated renewal of the aqueous transition metal solution [4,6].

A promising alternative for introducing transition metal cations into extra-framework positions of zeolites is the solid-state ion exchange technique. This method, first applied by Clearfield et al. [11], has attracted broad attention since about one decade. The state of the art has been reviewed recently by Karge [12]. Surprisingly, detailed investigations of the cation distributions in transition-metal-exchanged zeolites prepared this way do not seem to have been reported. The present contribution aims at elucidating this subject for the case of zinc exchange in zeolite Y. The characterization of the catalysts is performed with a combined technique of adsorption and NMR spectroscopy using carbon monoxide and xenon as probes. This analytical procedure has proven useful for the quantitative study of cation distributions in zinc- and cadmium-exchanged zeolites [4–6,13–16].

## 2. Experimental

$NH_4Y$ was obtained from commercially available zeolite $NH_4NaY$ (Y64, UOP, $Si:Al = 2.4$, $NH_4:Al = 0.85$) by repeated ion exchange with 1 mol $dm^{-3}$ aqueous $NH_4Cl$ solution under reflux conditions and subsequent washing with bidistilled water. The residual sodium content of $NH_4Y$ was determined by $^{23}Na$ NMR spectroscopy to correspond to $Na^+:Al < 0.05$.

Mixtures of $NH_4Y$ and crystalline $ZnCl_2$ with different mass ratios were prepared in an agate mortar and then transferred into glass tubes which were connected to a high vacuum and gas handling line. After evacuation at ambient temperature ($10^{-1}$ Pa), the samples were heated at a rate of 20 K/h to 120 °C maintained for 5 h, and subsequently

* To whom correspondence should be addressed.

at 40 K/h to 420 °C held for 24 h. The final vacuum was $p \leqslant 10^{-3}$ Pa. Samples prepared this way are designated Zn($\alpha$)HY, where $\alpha$ is two times the percental molar ratio of salt and framework aluminium in the precursor mixture. This definition implies that $\alpha$ is identical with the percentage of zinc for ammonium exchange in the event that $Zn^{2+}$ from the salt is completely ion-exchanged into the zeolite.

Zeolite Zn(135)HY was rehydrated at ambient atmosphere (7 days), washed repeatedly with bidistilled water at ambient temperature, and finally dehydrated again by heating in vacuo ($p \leqslant 10^{-3}$ Pa) at 400 °C (16 h). The designation of the resulting material is Zn(135)HYW.

Chemical analysis of the prepared samples with respect to their zinc and chloride content was performed with the aid of X-ray fluorescence spectroscopy (XRF) using the framework aluminium as an internal standard. The intensities of the K-lines of Zn, Cl, and Al served for the determination of Zn : Al and Cl : Al which were calibrated with standard samples of known atomic ratios.

Adsorption isotherms of nitrogen (−196 °C), carbon monoxide (25.0 °C), and xenon (25.0 °C) were measured volumetrically using all-steel devices. From the low-temperature $N_2$ adsorption isotherms the saturation capacities, $n^s(N_2)$, were determined and the pore volumes, $V_p$, calculated according to Gurvitch's rule [17].

The $^{129}$Xe NMR spectra of the encaged xenon atoms were measured at ambient temperature with an FT NMR spectrometer (CXP 100, Bruker, Karlsruhe, Germany) operating at the resonance frequency $\omega/2\pi = 21.4$ MHz. Depending on xenon loading, 500–50,000 FIDs were accumulated after $\pi/2$ pulse (3 $\mu$s) excitation with 1 s recycle delay before Fourier transformation was performed. Each of the measured spectra consisted of a single symmetric resonance line of full width at half height in the range of 3–8 ppm. The chemical shifts are quoted as $\delta = 10^6(\omega_{probe} - \omega_{ref})/\omega_{ref}$ with xenon gas at vanishing pressure used as the external reference.

## 3. Results

In table 1 are collected for each of the investigated samples (column 1) the concentration equivalents $N(ZnCl_2)$ of the salt contained in the precursor mixtures (column 2) as well as the concentrations $N$(J) (J = Zn and Cl) determined by XRF (columns 3 and 4). The concentrations are defined to be the number of species per unit cell (uc) of the zeolite. It is recognized that within the range of experimental error, the values of $N$(Zn) agree well with the figures of $N(ZnCl_2)$. The only exception is sample Zn(135)HYW, where $N$(Zn) is dinstinctly lower than $N(ZnCl_2)$.

Table 1
Chemical composition of samples and their precursor mixtures.

| Sample | $N(ZnCl_2)$ ($uc^{-1}$) | $N$(Zn)[a] ($uc^{-1}$) | $N$(Cl)[a] ($uc^{-1}$) |
|---|---|---|---|
| Zn(0)HY | 0 | 0 | 0 |
| Zn(25)HY | 7 | 8 | 0[b] |
| Zn(50)HY | 14 | 13 | 0[b] |
| Zn(75)HY | 21 | 22 | 0[b] |
| Zn(100)HY | 28 | 28 | 0[b] |
| Zn(135)HY | 38 | 38 | 25 |
| Zn(135)HYW | 38 | 28 | 0[b] |

[a] Estimated uncertainty: ±10%. [b] Below detection limit.

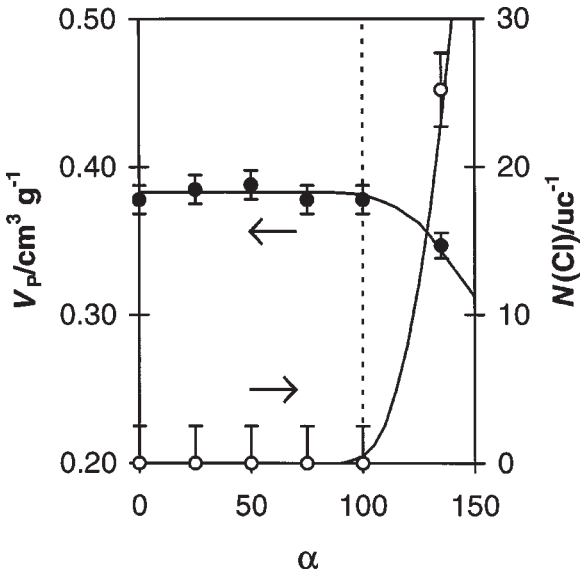


Figure 1. Micropore volume (•) and Cl content (○) of samples Zn($\alpha$)HY.

Figure 1 shows the micropore volume, $V_p$, and the concentration $N$(Cl) of the samples Zn($\alpha$)HY as function of the zinc chloride content of the corresponding precursor mixtures, $\alpha$. The micropore volume is found to be nearly independent of $\alpha$ up to $\alpha = 100$, but significantly decreases when $ZnCl_2$ is applied in excess ($\alpha = 135$). Concomitantly, the Cl content of the samples is zero at $\alpha \leqslant 100$, but steeply increases to about 25 $uc^{-1}$ (uc = unit cell) at $\alpha = 135$. Remarkably, $N$(Cl) is zero again after the washing procedure has been performed (table 1).

Figure 2 (a)–(c) shows the adsorption isotherms of carbon monoxide, the adsorption isotherms of xenon, and the $^{129}$Xe NMR chemical shifts $\delta$ of sorbed xenon, respectively, measured for zeolites Zn($\alpha$)HY ($\alpha$ = 0–100). The sample Zn(0)HY exhibits almost negligible CO adsorption, a linear adsorption isotherm of xenon, and a linear chemical shift versus pressure curve. In contrast, for $\alpha > 0$, the adsorption isotherms of both CO and Xe as well as the chemical shift curves show distinctly non-linear behaviour. Initially, the adsorption isotherms rise more or less steeply, and subsequently follow almost straight lines with slopes quite similar to those of the isotherms of Zn(0)HY. The chemical shift curves are displaced distinctly downfield (to higher $\delta$) from Zn(0)HY, and in each case decrease with increasing pressure running through flat minima at some higher value of $p$. The adsorbed amounts of both CO and Xe, as well as the chemical shifts, increase monotonously with $\alpha$ within the whole pressure range investigated.

Figure 3 (a)–(c) shows the adsorption isotherms of CO and Xe as well as the $^{129}$Xe NMR chemical shifts of the

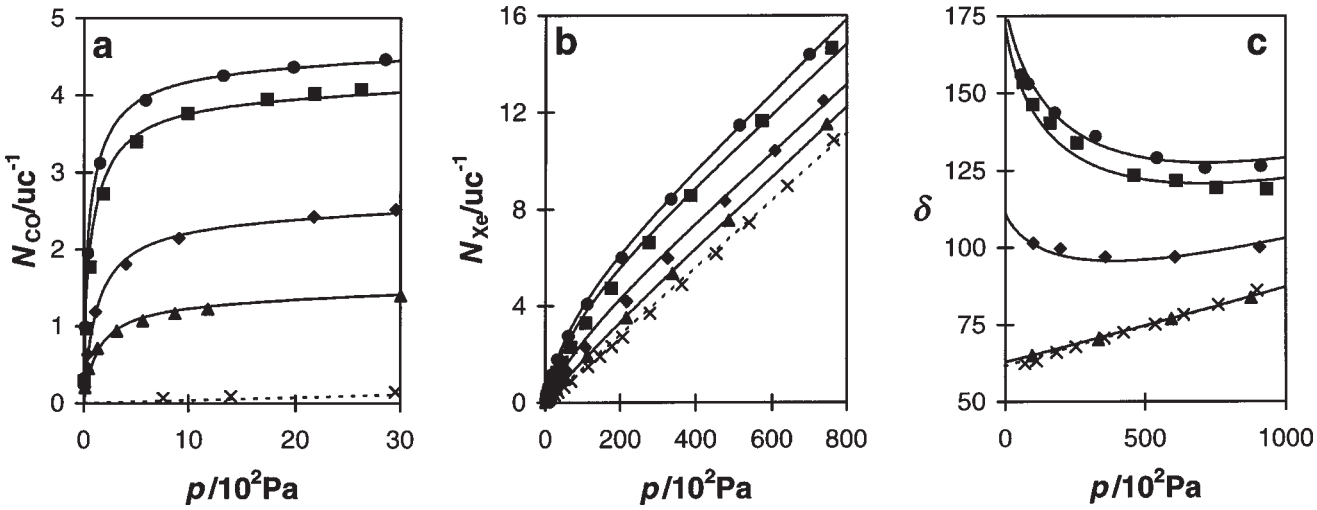


Figure 2. Adsorption isotherms of CO (a) and Xe (b) as well as $^{129}$Xe NMR chemical shifts (c) of sorbed xenon in zeolites Zn($\alpha$)HY: $\alpha$ =0 (×), 25 (▲), 50 (♦), 75 (■), 100 (●). Measuring temperature is 25 °C. The solid lines are fits as described in the text.

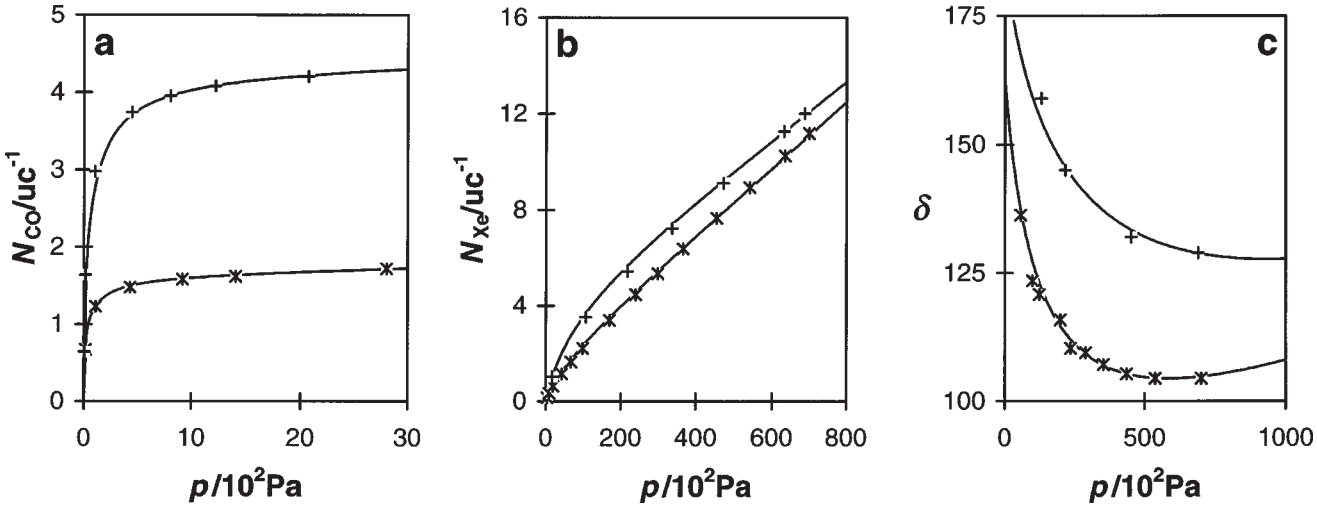


Figure 3. Adsorption isotherms of CO (a) and Xe (b) as well as $^{129}$Xe NMR chemical shifts (c) of sorbed xenon in zeolites Zn(135)HY (∗) and Zn(135)HYW (+). Measuring temperature is 25 °C. The solid lines are fits as described in the text.

encaged xenon atoms, respectively, obtained for the zeolites Zn(135)HY and Zn(135)HYW. The measured data lie on curves of similar character as observed for the materials with $\alpha \leqslant 100$ (figure 2 (a)–(c)). A closer inspection reveals that the adsorption isotherms and chemical shifts of sample Zn(135)HYW are in the vicinity of the corresponding curves of Zn(100)HY, whereas the non-washed zeolite Zn(135)HY exhibits significantly smaller CO and Xe adsorption as well as lower $^{129}$Xe NMR chemical shifts.

## 4. Discussion

### *4.1. Inferences from chemical analysis*

The results of the XRF analysis presented in table 1 enable us to draw several conclusions concerning the solid-state exchange process. The observation that in the case of the samples Zn($\alpha$)HY with $\alpha \leqslant 100$ the concentration of Cl, $N$(Cl), is zero, and the concentration of Zn, $N$(Zn), is just the same as $N(ZnCl_2)$ of the precursor mixture, is clear evidence that the solid-state reaction

$$2NH_4^+(\text{zeolite}) + ZnCl_2\ (\text{cryst.}) \longrightarrow Zn^{2+}(\text{zeolite}) + 2NH_3\ (\text{gas})\uparrow + 2HCl\ (\text{gas})\uparrow \quad (1)$$

has taken place till complete consumption of the applied salt. These results also indicate that a conceivable escape of $ZnCl_2$ by sublimation (equilibrium vapour pressure of $ZnCl_2$ at 420 °C is 170 Pa [18]) cannot have occurred to an appreciable extent since otherwise the agreement of $N$(Zn) with $N(ZnCl_2)$ (table 1) could not be explained.

Turning to sample Zn(135)HY it is reasonable to assume that, as in the case of Zn(100)HY, reaction (1) has proceeded to complete conversion of the zeolitic $NH_4^+$ cations. This assumption implies that the observed XRF signal of Cl is due to unreacted $ZnCl_2$ residing either within the micropores or at the outer surface of the zeolite crystallites. In

either case, the concentration of the residual salt should correspond to $(1/2)N$(Cl), i.e., to about 13 $ZnCl_2$/uc (table 1). Since the overall zinc concentration of zeolite Zn(135)HY detected by XRF is $N$(Zn) = 38 Zn/uc (table 1), the concentration of $Zn^{2+}$ incorporated into extraframework sites in this material should be 25 $Zn^{2+}$/uc. Within experimental error, this figure agrees with $N$(Zn) of sample Zn(100)HY (table 1) verifying the a priori introduced suggestion of a complete consumption of $NH_4^+$.

The washing process leading to sample Zn(135)HYW is expected to remove the surplus $ZnCl_2$ completely, both from the outer surface of the zeolite crystallites as well as from the supercages [19,20]. In any case, by washing of sample Zn(135)HY the concentrations $N$(Zn) and $N$(Cl) should be reduced to about 25 Zn/uc and 0 Cl/uc, respectively, which, in fact, is observed (table 1). At least part of the residual salt contained in sample Zn(135)HY must be considered to reside in the supercages because otherwise the reduction of pore volume (figure 1) could not be understood.

From the discussion carried out so far, the picture emerges that heating $NH_4Y/ZnCl_2$ mixtures at 420 °C under high vacuum transfers quantitatively the zinc cations from the salt into the zeolite as far as ammonium ions or protons (if $NH_4^+$ is decomposed prior to the reaction with $ZnCl_2$) are available for exchange. Surplus zinc chloride contained in the precursor mixture is, at least in part, incorporated in the supercages of the zeolite structure. The interesting and most important question with respect to catalytic application concerns the distribution of the zinc cations in the so prepared samples between the small and large cages, and between the crystallographic sites SIII and SII in the latter.

### 4.2. Quantitative $^{129}$Xe NMR spectroscopy

It is known that due to their size carbon monoxide and xenon cannot penetrate into the small cavities of the faujasite ($\beta$-cage/hexagonal prism units), which circumstance makes them ideal probes for the investigation of the chemical properties of the supercages of zeolite Y. In previous papers, it was demonstrated that the method of quantitative $^{129}$Xe NMR spectroscopy, comprising the measurement of the adsorption isotherms of CO and Xe, and of the $^{129}$Xe NMR chemical shifts of encaged xenon atoms, allows to obtain information about the cation distributions referred to before [4–6,13–16]. The well-proven model underlying the analysis of the experimental data assumes localized (Langmuir-type) adsorption of CO and Xe at the transition-metal cations located at the crystallographic SIII and SII positions, and non-localized (Henry-type) adsorption of both probes at the residual internal surface. This model yields the expressions [4–6,13–16]

$$N_{\mathrm{J}} = \frac{n_1 k_1^{\mathrm{J}} p}{1 + k_1^{\mathrm{J}} p} + \frac{n_2 k_2^{\mathrm{J}} p}{1 + k_2^{\mathrm{J}} p} + K_{\mathrm{H}}^{\mathrm{J}} p, \tag{2}$$

Table 2
Site-characteristic adsorption and NMR parameters ($T$ = 298 K).

| $i$ | Adsorption site | $k_i^{\mathrm{CO}}$ ($\times 10^{-2}$ Pa$^{-1}$) | $k_i^{\mathrm{Xe}}$ ($\times 10^{-2}$ Pa$^{-1}$) | $\delta_i$ |
|---|---|---|---|---|
| 1 | $Zn^{2+}$ (SIII) | 13 | 0.023 | 220–235 |
| 2 | $Zn^{2+}$ (SII) | 0.74 | 0.008 | 130–140 |

describing the total adsorption of J (CO or Xe), $N_{\mathrm{J}}$, as function of the equilibrium pressure $p$, and

$$\delta = \frac{1}{N_{\mathrm{Xe}}}\left[\frac{n_1 k_1^{\mathrm{Xe}} p}{1 + k_1^{\mathrm{Xe}} p}\delta_1 + \frac{n_2 k_2^{\mathrm{Xe}} p}{1 + k_2^{\mathrm{Xe}} p}\delta_2 + K_{\mathrm{H}}^{\mathrm{Xe}} p \delta_{\mathrm{H}}\right] + F N_{\mathrm{Xe}}, \tag{3}$$

describing the isotropic chemical shift $\delta$ of xenon in the rapid exchange limit. In equations (2) and (3), $n_1$ and $n_2$ are the concentrations of the particular adsorption sites (index 1: $Zn^{2+}$ at SIII; index 2: $Zn^{2+}$ at SII); $k_i^{\mathrm{J}}$ are the Langmuir adsorption constants of probe J and $\delta_i$ the local isotropic chemical shift of xenon associated with the corresponding type of site $i$ ($i = 1, 2$). $K_{\mathrm{H}}^{\mathrm{J}}$ and $\delta_{\mathrm{H}}$ are the Henry adsorption constant of J and the chemical shift of xenon at the residual internal zeolite surface, respectively. $FN_{\mathrm{Xe}}$ is an empirical term taking into account mutual magnetic xenon–xenon interactions with the value $F$ = 1.87 ppm uc which is typical of xenon in faujasite-type materials [4–6,13–16].

The parameters $k_i^{\mathrm{J}}$ and $\delta_i$ ($i = 1, 2$; J = CO, Xe) are considered to be site-specific. Therefore, these quantities are required to have the same values in the present investigation of solid-state zinc-exchanged zeolites Y as were found previously for similar materials prepared by the techniques of wet exchange [4–6] and chemical vapour deposition [4,13,14]. The site-specific parameters (table 2) were taken over from [4,5]. The fitting of the experimental data to equations (2) and (3) requires to find values for the concentrations $n_1$ and $n_2$ as well as for $K_{\mathrm{H}}^{\mathrm{J}}$ and $\delta_{\mathrm{H}}$.

The solid curves in figures 2 and 3 show the optimum fits obtained with the preset data of table 2 and the values of the adjustable parameters collected in table 3. The fits were performed with a trial and error procedure with which simultaneously best fits of the data sets of the three independently measured quantities were achieved. Obviously, the experimental adsorption data of both CO and Xe, as well as the chemical shifts of xenon, are very well reproduced. It is noted that for the zeolite with the lowest zinc content, Zn(25)HY, the displayed fitting curves in figure 2 were obtained with $k_2^{\mathrm{Xe}} = 3 \times 10^{-5}$ Pa$^{-1}$ and $\delta_2$ = 80 ppm, which are significantly lower than the corresponding data listed in table 2. A comment to this surprising finding will be given below.

Of the data collected in table 3, the values of the concentrations of $Zn^{2+}$ ions on sites SIII and SII, $n_1$ and $n_2$, are of most interest, and we will therefore focus the discussion on them. In figure 4, the values of $n_1$ and $n_2$, as well as of the total $Zn^{2+}$ concentrations in the supercages, $n_1 + n_2$, are displayed as function of $\alpha$. The figure also contains the

Table 3
Sample-characteristic parameters ($T = 298$ K).

| Sample | $n_1$ ($uc^{-1}$) | $n_2$ ($uc^{-1}$) | $K_H^{CO}$ ($\times 10^{-5}$ $uc^{-1}$ $Pa^{-1}$) | $K_H^{Xe}$ ($\times 10^{-4}$ $uc^{-1}$ $Pa^{-1}$) | $\delta_H$ |
|---|---|---|---|---|---|
| Zn(0)HY = HY | 0 | 0 | 3.6 | 1.43 | 61 |
| Zn(25)HY | 0.0 | 1.35 | 3.6 | 1.41 | 58 |
| Zn(50)HY | 0.1 | 2.4 | 4.0 | 1.38 | 64 |
| Zn(75)HY | 1.4 | 2.65 | 3.4 | 1.40 | 68 |
| Zn(100)HY | 1.95 | 2.5 | 3.6 | 1.48 | 70 |
| Zn(135)HY | 1.0 | 0.65 | 3.4 | 1.37 | 68 |
| Zn(135)HYW | 1.8 | 2.5 | 3.6 | 1.18 | 71 |

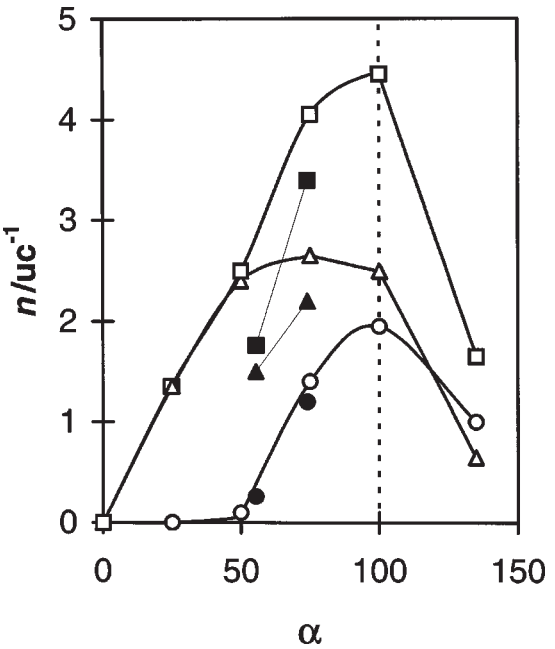


Figure 4. Concentrations of $Zn^{2+}$ cations at supercage positions within samples Zn($\alpha$)HY (open symbols) and Zn($\alpha$)NaY (closed symbols): SIII (○, ●), SII (△, ▲), SIII + SII (□, ■).

corresponding data published previously for the zeolites Zn($\alpha$)NaY which were obtained from NaY (Union Carbide, LZ-Y52, Si : Al = 2.4) by the conventional wet ion exchange technique [6]. Here, $\alpha$ is the degree of zinc for sodium exchange as determined by chemical analysis [6].

Several interesting information can be gained from figure 4. (i) In both the wet and the solid-state ion-exchanged samples, the zinc cations show strong preference for the small cages, i.e., the concentrations $n_1 + n_2$ are small compared to the total zinc content of the materials (table 1). (ii) In the solid-state exchanged zeolites the sites SII become populated almost exclusively up to $\alpha = 50$, whereas at higher overall exchange the concentration of $Zn^{2+}$ on these sites remains almost constant, and the further increase of the supercage $Zn^{2+}$ ions up to $\alpha = 100$ comes from the population of sites SIII. These findings are of interest in view of the presumed catalytic activity of the latter cationic sites. In the samples obtained by the wet exchange the concentration of zinc ions on SIII exhibit a similar behaviour, but here the expected maximum concentration cannot be obtained because of the difficulty to achieve complete replacement of $Na^+$ by $Zn^{2+}$ with this exchange technique. (iii) The drastic reduction of both $n_1$ and $n_2$ in zeolite Zn(135)HY is certainly due to the zinc chloride occluded in the supercages at $\alpha > 100$. Most probably, the salt forms charged complexes of the type $[Zn_yCl_{2y-x}]^{x+}$ with $Zn^{2+}$ cations on both SII and SIII positions, so that these cations are no longer accessible to CO and Xe. Clusters of similar type, $[Na_yHal_{y-x}]^{x+}$, have previously been reported for zeolite NaY loaded with sodium halides (NaHal) [19,20]. The suggestion of complex formation is corroborated by the observation that after removal of the salt from the supercages (Zn(135)HYW), the values of $n_1$ and $n_2$ as in Zn(100)HY are almost restored again (table 3).

Finally, we comment on the unusual behaviour of xenon in sample Zn(25)HY, i.e., the significant deviatons of $k_2^{Xe}$ and $\delta_2$ from the standard values to be found in table 2. First, it is stated that the figures in the table were derived exclusively from investigations of zeolites Y with degrees of zinc exchange >50%. A possible explanation of these findings can be given as follows. The exact position of the zinc cations, on SII say, is expected to be determined by electrostatics which depends on the arrangement of the surrounding charges. The positive charge accumulated in the $\beta$-cages due to the preference of the $Zn^{2+}$ is conceivable to cause some displacement of the $Zn^{2+}$ cations at SII towards the supercages at high in comparison to low degree of ion exchange. For the materials with low $Zn^{2+}$ content, this implies a larger cation–xenon distance and, hence, a smaller Coulomb field at the xenon atom. According to a recent theoretical study showing that the polarization interaction determines both the potential energy and the isotropic chemical shift of xenon in a cation/xenon complex [21], the above-mentioned decrease of the Coulomb field should result in a weaker adsorption of xenon and a smaller chemical shift value. Actually, this is what is experimentally observed.

## 5. Conclusion

In the present study, it has been demonstrated that the zinc cations of crystalline zinc chloride mixed with zeolite $NH_4Y$ can quantitatively be transferred into the alumino–silicate material up to complete consumption of the am-

monium ions. Surplus salt in the precursor mixture is incorporated in the supercages, affecting the accessibility and, hence, the interaction of the charge compensating zinc cations with CO and Xe. Most probably, also the access of reactant molecules of interest for catalytic conversions becomes restricted. Maximum concentration of accessible $Zn^{2+}$ sites is achieved with a salt/zeolite mixture containing the components in the molar ratio $Zn^{2+} : Al = 1 : 2$.

## Acknowledgement

Financial support by Deutsche Forschungsgemeinschaft (Schwerpunktprogramm "Nanostrukturierte Wirt/Gast-Systeme") is gratefully acknowledged.

## References

[1] I.E. Maxwell, Adv. Catal. 31 (1982) 1.
[2] Y. Ono, Catal. Rev. Sci. Eng. 34 (1992) 179.
[3] A. Hagen and F. Roessner, Stud. Surf. Sci. Catal. 83 (1994) 313.
[4] A. Seidel, Lewis-Säurezentren in synthetischem Faujasit – Eine Fallstudie am Beispiel zink- und protonenhaltiger Y-Zeolithe, Ph.D. thesis, University of Dortmund (Shaker, Aachen, 1997).
[5] A. Seidel, F. Rittner and B. Boddenberg, J. Chem. Soc. Faraday Trans. 92 (1996) 493.
[6] B. Boddenberg and A. Seidel, J. Chem. Soc. Faraday Trans. 90 (1994) 1345.
[7] A.P. Wilkinson, A.K. Cheetham, S.C. Tang and W.J. Reppart, J. Chem. Soc. Chem. Commun. (1992) 1485.
[8] P.B. Peapples-Montgomery and K. Seff, J. Phys. Chem. 96 (1992) 5962.
[9] K. Otsuka, J. Manda and A. Morikawa, J. Chem. Soc. Faraday Trans. 1 77 (1981) 2429.
[10] T.A. Egerton and F.S. Stone, J. Chem. Soc. Faraday Trans. I 69 (1973) 22.
[11] A. Clearfield, C.H. Saldarriaga and R.C. Buckley, in: *Proc. 3rd Int. Conference on Molecular Sieves, Recent Progress Reports*, ed. J.B. Uytterhoeven (Leuven University Press, Leuven, 1973) p. 241.
[12] H.G. Karge, Stud. Surf. Sci. Catal. 105 (1997) 1901.
[13] F. Rittner, A. Seidel, T. Sprang and B. Boddenberg, Appl. Spectrosc. 50 (1996) 1389.
[14] A. Seidel and B. Boddenberg, Chem. Phys. Lett. 249 (1996) 117.
[15] T. Sprang, A. Seidel, M. Wark, F. Rittner and B. Boddenberg, J. Mater. Chem. 7 (1997) 1429.
[16] B. Boddenberg and T. Sprang, J. Chem. Soc. Faraday Trans. 91 (1995) 163.
[17] S.J. Gregg and K.S.W. Sing, *Adsorption, Surface Area and Porosity* (Academic Press, London, 1982).
[18] O. Knacke, O. Kubaschewski and K. Hesselmann, *Thermodynamical Properties of Inorganic Substances*, 2nd Ed. (Springer, Berlin, 1991).
[19] A. Seidel, U. Tracht and B. Boddenberg, J. Phys. Chem. 100 (1996) 15917.
[20] J.A. Rabo, in: *Zeolite Chemistry and Catalysis*, ACS Monograph, Vol. 171, ed. J.A. Rabo (Am. Chem. Soc., Washington, DC, 1976) p. 332.
[21] A. Freitag, Ch. van Wüllen and V. Staemmler, Chem. Phys. 192 (1995) 267.